4.8 HIGH-HEAT FLUX TESTING OF LOW-LEVEL IRRADIATED MATERIALS USING PLASMA ARC LAMPS - A.S. Sabau, L.L. Snead, Y. Katoh (Oak Ridge National Laboratory), Kazutoshi Tokunaga (Kyushu University, Japan)

OBJECTIVE

The objective of this work, part of the PHENIX collaboration with Japan, is testing of irradiated materials that are candidate divertor component materials and mock-up divertor components under high-heat flux using Plasma Arc Lamps (PAL).

SUMMARY

In this reporting period, high-heat flux testing of five specimens, supplied by the Japanese collaborators in the PHENIX program, was conducted at ORNL. Dr. Tokunaga was on assignment at ORNL for four weeks as part of the joint US/Japan PHENIX program, during which time this high-heat flux testing and evaluation of the clamping fixture and vacuum system was conducted.

PROGRESS AND STATUS

Effort was conducted in three main areas: (a) reducing the oxidation of the specimen during high-heat flux testing and implicitly enhancing the radiation safety during testing of irradiated specimens, (b) achieving a high thermal gradient through the specimen while enhancing the measurement accuracy of the specimen temperature, and (c) conducting high-heat flux testing with non-irradiated samples as part of the joint US/Japan PHENIX program.

Reduction in the oxidation and enhancing the radiation safety

The reduction in the oxidation during testing of irradiated specimens was accomplished by employing an additional high-vacuum test section embedded within the main test chamber (low-vacuum). The high-vacuum test section would enclose the cooling rod, holder, and irradiated sample (Fig 1a). The main test chamber will not be contaminated, lowering the maintenance and operational costs. Also, the limited amount of O_2 in the high-vacuum test section will severely limit formation of tungsten oxide on the irradiated sample. Specifically, the high-vacuum section is made by a quartz dome, whose circumference is shielded by a Cu plate in order to protect the O-ring seal from direct heating by the plasma-arc lamp (Fig. 1b).

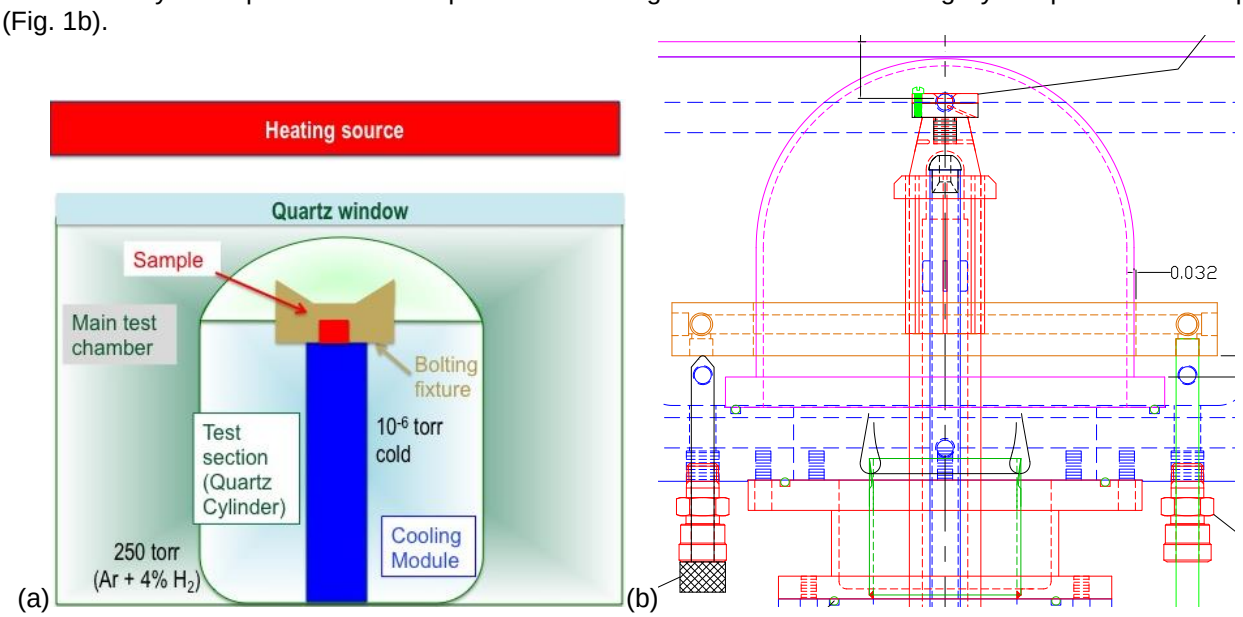

Figure 1. Schematic illustrating the use of two confinement enclosures in the test section.

High-thermal gradient during HHFT

In order to attain a high thermal gradient through the samples, new bolting holders were fabricated from a Ta10W alloy that exhibits high strength at high temperature. In the final design, as shown in Figure 2, the specimen was mounted directly onto a Cu cooling rod to attain the lowest temperature on the back surface of the specimen and thus enabling the highest thermal gradient in the specimen. Pictures of the actual setup are shown in Figure 3. The thermocouple wires were shielded by a Nb cone.

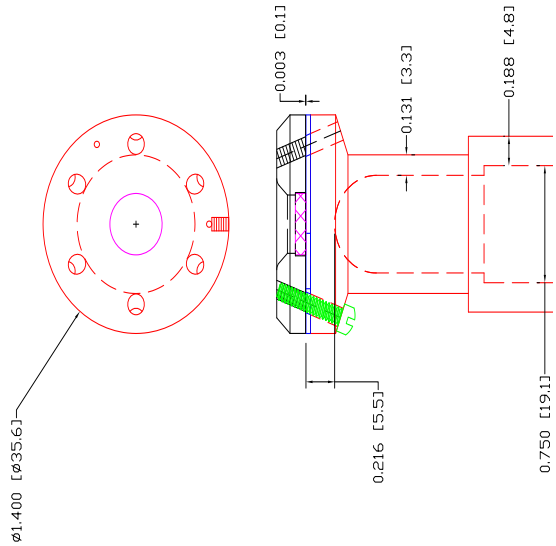

Figure 2. Drawing of the final design for the cooling rod and bolting fixture.

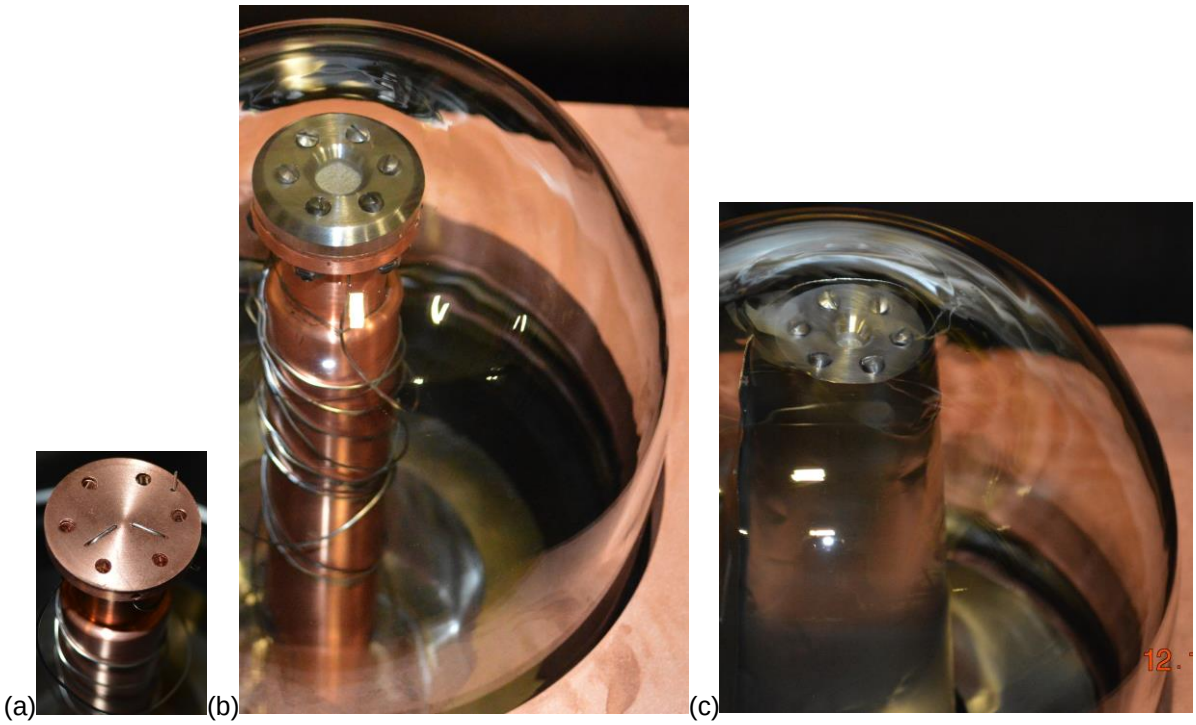

Figure 3. Thermocouples mounting: (a) top view of washer showing 2 thermocouples that will be sandwiched between Cu rod and specimen, (b) view of specimen 1 and bolting flange through quartz dome and unshielded thermocouple wires, (c) view of specimen 5, bolting flange, Nb cone (shielding the thermocouple wires) through quartz dome.

High-heat flux experiments

Several high-heat flux experiments were conducted during the December visit of Dr. Kazutoshi Tokunaga of Kyushu University as part of the joint US/Japan PHENIX program. Five W/F82H specimens, which were supplied by the Japanese collaborators in the PHENIX program, were exposed to high-heat fluxes at ORNL (Table 1). Thickness of W and F82H steel was 1 mm, each. Each specimen was exposed to corresponding high-heat fluxes such that the maximum temperature would attain the target temperature shown in Table 1. During high-heat flux testing, a non-uniform temperature is expected in the specimen. The specimen temperature was measured with thermocouples inserted between the back surface of the specimen and top surface of Cu rod, $T_{BS, Cu}$. The data for the high-vacuum pressure and $T_{BS, Cu}$ is next shown for selected cycles for specimens 1, 2 and 5.

Table 1. W/F82H specimens exposed to high-heat flux testing.

	Diameter [mm]	[1]Target Max. Temp. [^oC]	[2]No. of Cycles	[3]Cycle duration [s]	Max. Heat Flux [W/cm^2]	Comments
1	10	750	101	10-15	300	Delamination observed
2	10	500	164	7-10	210-278	No delamination observed (Visual)
3	10	550	214	4-5	300	No delamination observed (Visual)
4	6	450	110	10-16	300	No delamination observed (Visual)
5	6	550	42	10-15	300-323	[4]No delamination observed (Visual)

[1] The target temperature for the interface between the W and F82H.
[2] Number of cycles at heat flux.
[3] Thickness W and F82H steel was 1 mm each.
[4] Shielded thermocouples from the direct IR flux

In order to keep the vacuum pressure to acceptable levels, the heat flux was increased incrementally to its maximum value. Data acquired with a high-vacuum pressure transducer indicated that the absolute pressure increased during the HHFT (Figures 4a and 4c). The temperature is shown in Figures 4b and 4d for specimen 1 for cycles 84-85 and 132-134, respectively. For specimen 1, $T_{BS, Cu}$ temperatures higher than 600°C were measured when the high-heat flux exposure was increased from 12 s to 15 s (cycles 132-134).

The pressure and temperature data is shown for specimen 2 in Figure 5. The maximum pressure was approximately 10^{-4} Torr, higher than that for specimen 1. This higher vacuum was maintain for all the subsequent specimens, indicating that the entire testing section was preconditioned during the HHFT of specimen 1 by slowly evolving most of the volatile species in the test section. The peak heat fluxes for specimen 2 were lower than those for specimen 1 in order to keep the measured temperature $T_{BS, Cu}$ below 500°C.

The pressure and temperature data is shown for specimen 5 in Figure 6. The temperature data for specimens 1 and 2 (Figures 4b, 4d, and 5b) was obtained with unshielded thermocouples while the temperature data for specimen 5 (Figure 6b) was obtained with shielded thermocouples. The peak of the measured temperature $T_{BS, Cu}$ was approximately 240°C. An analysis of this temperature data is being conducted to understand the effects of: (a) contact area between the thermocouple sheath with both back surface of specimen and cooling rod, and (b) shielding of the thermocouple wires in a region away from the thermocouple bead, the junction at which the temperature is actually measured. The temperatures at the top surface of the specimen are expected to be higher than measured temperature $T_{BS, Cu}$.

Profilometry measurements were conducted before and after HHFT. The specimens were flat before HHFT. The post-HHFT profilometry data indicated that the specimens bowed, raising the center of the W above its edge. The profilometry data was used to obtain the height of the center of the samples and it is shown in Table 2. The data showed that the 10 mm diameter specimens (i.e., specimens 1, 2, and 3) bowed more than 6 mm diameter specimens (i.e., specimens 4 and 5). The profilometry data is useful to

obtain the residual stresses in the specimens and further validate the maximum temperature conditions during HHFT.

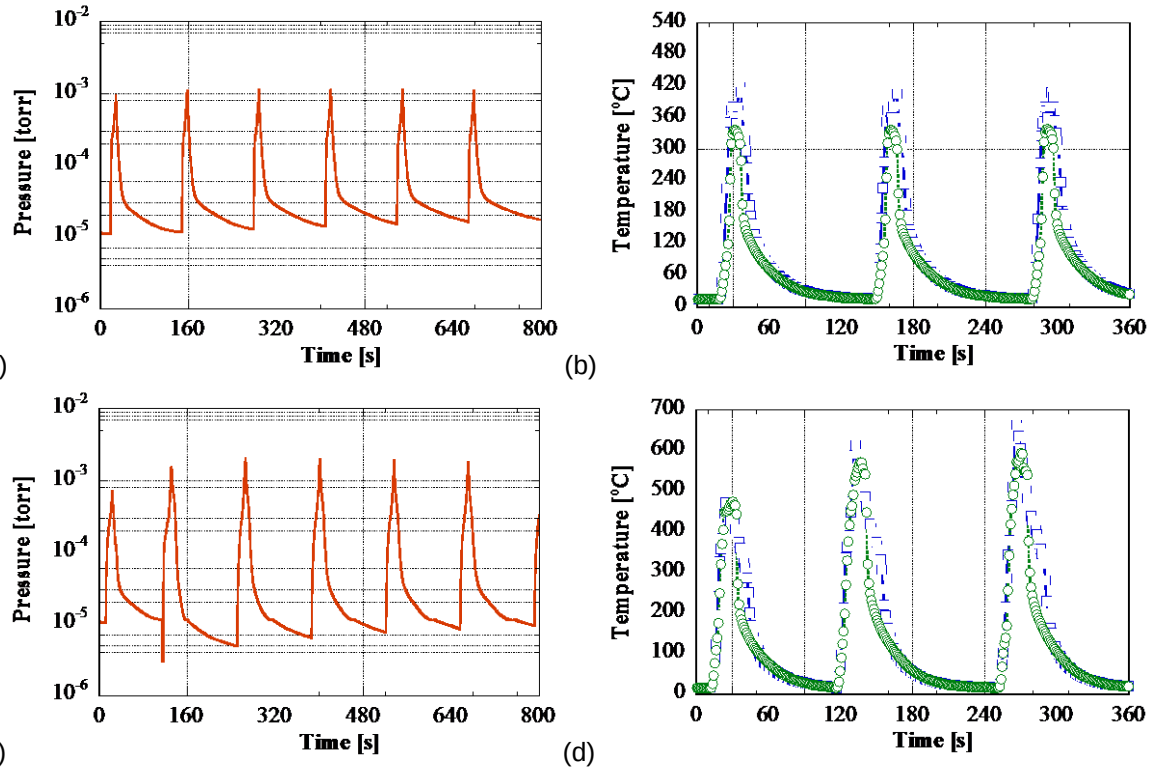

Figure 4. Representative data for specimen 1: (a) absolute pressure for cycles 84-89 (300 W/cm^2 for 10 s) and (b) measured temperature $T_{BS,\ Cu}$ for cycles 84-85 with un-shielded thermocouples, (a) absolute pressure for cycles 132-137 and (b) measured temperature $T_{BS,\ Cu}$ for cycles 132-134 (300 W/cm^2 for 12 s cycle 132 and 15 s for cycles 133-137).

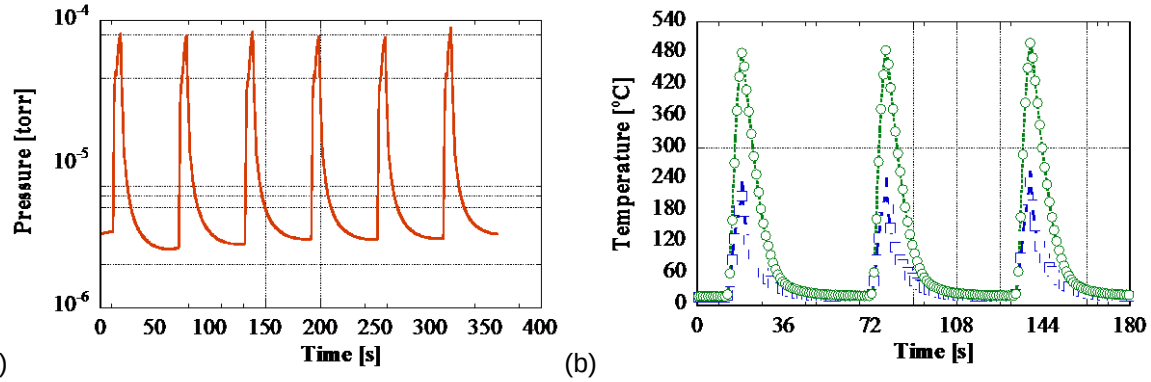

Figure 5. Representative data for specimen 2: (a) absolute pressure for cycles 114-119 and (b) measured temperature $T_{BS,\ Cu}$ for cycles 114, 115, and 116 with un-shielded thermocouples (each cycle: 278 W/cm^2 for 7 s).

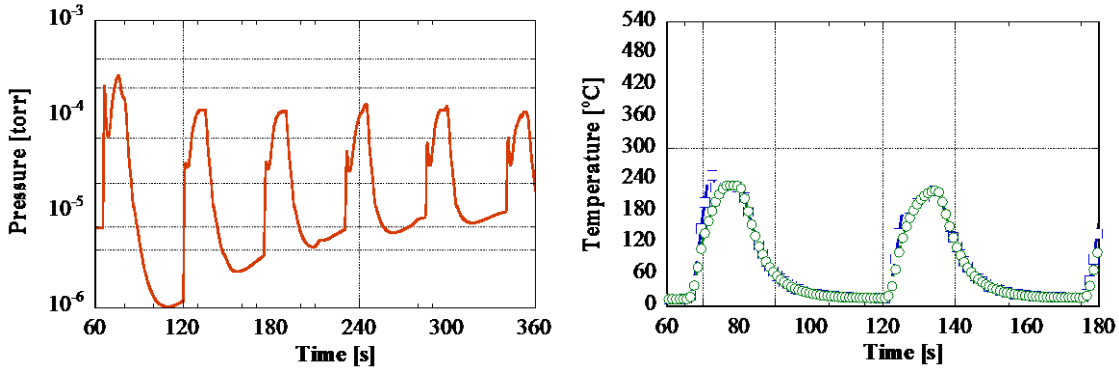

Figure 6. Representative data for specimen 5: (a) absolute pressure for cycles 37-42 and (b) measured temperature $T_{BS,\ Cu}$ for cycles 37 and 38 with shielded thermocouples (each cycle: 323 W/cm^2 for 15 s).

Table 2. Height of the center of the sample [µm] with respect to the edge of the specimen in two orthogonal directions.

Sample	X	Y
1	31.1	53.2
2	41.3	49.2
3	33.1	45.1
4	8.2	19.9
5	3.5	26.3

Acknowledgments

The authors would like to thank Evan Ohriner for material selection based on strength, oxidation, and fabrication considerations, Charles Ross (Chuck) Schaich for assisting with CAD design, fabrication specifications, and assembly; Jim Kiggans for design and fabrication of the Al enclosure, David Harper for operating the PAL, and John Henry Jr. for conducting profilometry measurements. We would also like to acknowledge the following Japanese collaborators from the joint US-Japan PHENIX program, Y. Ueda of Osaka University, Japan for numerous discussions related to clamping and T. Yokomine of Kyoto University, Japan for presentations made as part of the PHENIX program, discussing high-heat flux testing of He cooled tungsten.